SUPPLEMENTARY MATERIALS

Analytical Techniques

Fresh >2 kg samples free from silica or carbonate veining were collected from outcrops on the island of Innersuartuut (Supplementary Figure 1 and Supplementary Table 1) using a sledgehammer. Clean, interior pieces were coarsely crushed using a hydraulic press, with a representative split powdered in an Al_2O_3 swing mill. Major element compositions were determined by standard XRF methods at Geoscience Australia using a Philips PW2404 sequential spectrometer, using methods described in Jenner et al. (2009). For trace element analyses, fused glass discs were prepared using a high purity $LiBO_3$ flux and a 3:1 flux to sample ratio. $LiBO_3$ discs were analysed at the Research School of Earth Sciences, ANU, using a quadrupole ICP-MS (7500S Agilent; RF power = 1200 W; ablation cell gas flow = 0.3 litres min^{-1} He, 0.02 litres min^{-1} H_2; auxiliary gas flow = 1.0 litres min^{-1} Ar; laser energy = 50-55 mJ) coupled to a 193 nm Excimer (Lambda Physik LPX 120i) laser ablation system. NIST SRM 612 was used for external calibration of data, using preferred values listed in Jenner and O'Neill (2012b). Analytical data, precision and accuracy for replicate analyses of international reference materials are given in Supplementary Table 2. Analytical precision is typically less than or equal to 2-3% RSD (1σ relative standard deviation) as determined by replicate analyses of references materials BIR-1, AGV-2, W-2 and BHVO-2. Accuracy of analyses are typically within $\leq$5% of preferred values (given in Supplementary Table 2) previously compiled on the GeoRem website (Jochum et al., 2005). Major and Trace element analyses of samples from Innersuartuut are given in Supplementary Table 3.

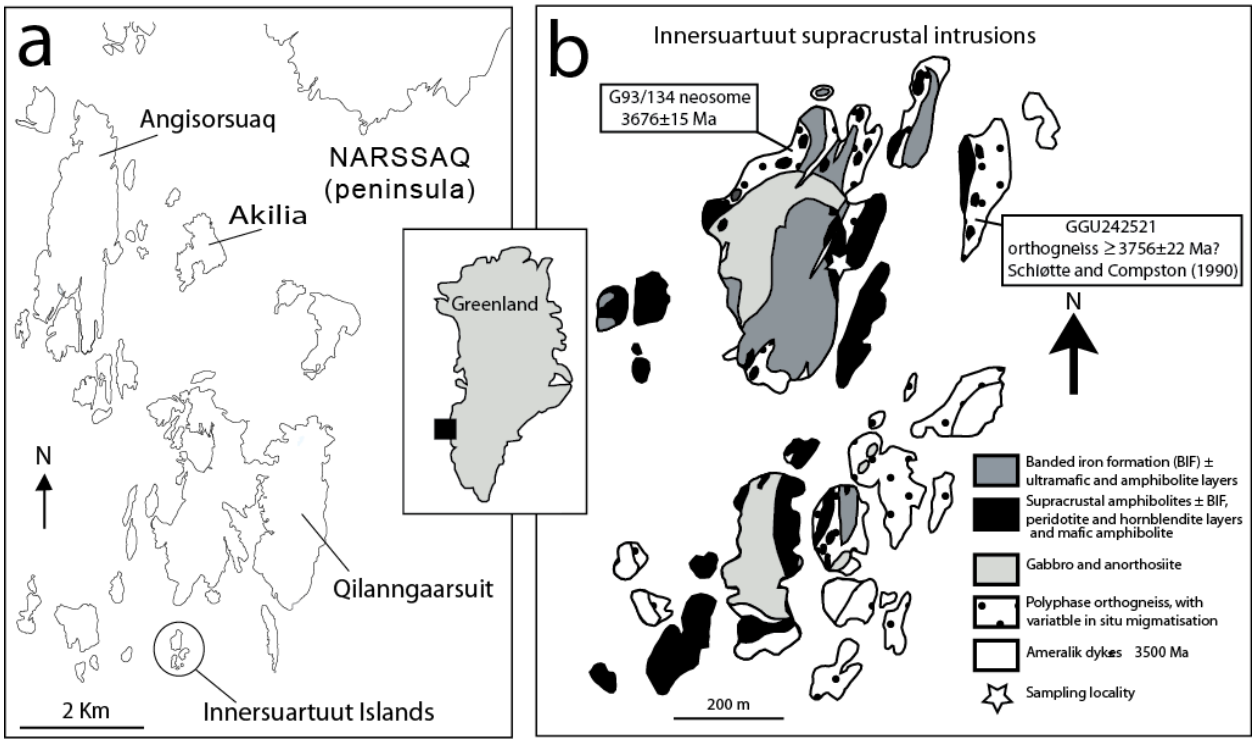

Supplementary Figure DR1: a) Map showing the the Nuuk region, West Greenland and the location of Innersuartuut islands; b) Simplified geological sketch map of Innersuartuut islands and the sample locality (maps modified from Nutman et al., 2002).

Supplementary Table DR1: Locations of samples (all using WGS84 datum).

Sample Name	Latitude	Longitude
JG03-27	63°50.323'N	51°40.936'W
JG03-29	63°50.287'N	51°40.894'W
JG03-30	63°50.287'N	51°40.894'W
JG03-31	63°50.259'N	51°40.880'W
JG03-32	63°50.259'N	51°40.880'W
G93-138 G93-140 G93-143 G93-144 G93-145 G93-146	63°50.259'N All G93 samples were collected within a 20meter radius of these coordinates.	51°40.880'W

Supplementary Table DR2: Preferred values for NIST SRM 612 used for external calibration and replicate analyses of reference materials used to monitor data quality

	NIST SRM	**BIR-1**				**AGV-2**				**W-2**				**BHVO-2**			
	612	**n=5**	%RSD	PV	R-value	**n=5**	%RSD	PV	R-value	**n=6**	%RSD	PV	R-value	**n=5**	%RSD	PV	R-value
Sc	39.9	**43.6**	1.70	43	1.01	**13.5**	2.50	13	1.04	**35.9**	1.259	35.9	1.00	**32.3**	1.22	32	1.01
Ti	39.4	**5743**	2.41	5600	1.03	**6048**	1.62	6287	0.96	**6439**	1.731	6347	1.01	**16566**	1.85	16300	1.02
Cr	39	**394**	1.44	391	1.01	**21.1**	1.49	16	1.32	**94.2**	0.882	93	1.01	**292**	0.54	280	1.04
Ni	38.8	**167**	0.28	166	1.00	**19.1**	2.96	20	0.95	**69.1**	0.263	72	0.96	**115**	0.41	119	0.97
Rb	31.4	**0.249**	3.28	0.2	1.24	**57.8**	0.74	66.3	0.87	**17.5**	0.506	21	0.83	**8.05**	0.60	9.11	0.88
Sr	78.4	**106**	0.52	109	0.97	**625**	0.60	661	0.95	**191**	0.703	196	0.97	**392**	0.29	396	0.99
Y	38.3	**14.4**	1.03	15.6	0.92	**17.7**	0.65	19	0.93	**19.9**	0.461	22	0.91	**24.2**	0.32	26	0.93
Zr	37.9	**13.9**	1.45	14	0.99	**217**	0.81	230	0.95	**90.9**	0.564	92	0.99	**165**	0.24	172	0.96
Nb	38.9	**0.527**	2.07	0.55	0.96	**13.4**	1.19	14.5	0.92	**7.13**	1.337	7.5	0.95	**17.8**	1.07	18.1	0.99
Ba	39.3	**6.45**	0.87	7.14	0.90	**1083**	0.53	1130	0.96	**167**	0.939	172	0.97	**127**	1.18	131	0.97
Hf	36.7	**0.563**	3.12	0.582	0.97	**4.93**	1.21	5	0.99	**2.46**	2.713	2.45	1.00	**4.29**	1.72	4.36	0.98
Ta	37.6	**0.035**	6.76	0.036	0.98	**0.767**	2.75	0.87	0.88	**0.433**	1.512	0.47	0.92	**1.09**	2.24	1.14	0.95
Th	37.79	**0.032**	10.60	0.032	1.01	**6.10**	0.41	6.1	1.00	**2.26**	1.412	2.17	1.04	**1.27**	2.26	1.22	1.04
U	37.38	**0.016**	6.06	0.010	1.55	**1.75**	1.84	1.86	0.94	**0.497**	2.859	0.51	0.98	**0.408**	3.86	0.403	1.01
La	36	**0.711**	2.74	0.615	1.16	**37.9**	0.43	37.9	1.00	**11.0**	0.367	10.8	1.02	**15.9**	0.81	15.2	1.05
Ce	38.4	**1.85**	1.08	1.92	0.96	**66.0**	1.04	68.6	0.96	**22.7**	0.515	23.4	0.97	**36.6**	0.61	37.5	0.98
Pr	37.9	**0.363**	1.54	0.37	0.98	**7.71**	0.73	7.84	0.98	**2.95**	0.468	3	0.98	**5.22**	0.97	5.35	0.98
Nd	35.5	**2.37**	1.72	2.38	1.00	**29.5**	0.43	30.5	0.97	**13.0**	0.913	13	1.00	**24.5**	0.63	24.5	1.00
Sm	37.7	**1.12**	0.97	1.12	1.00	**5.44**	1.40	5.49	0.99	**3.33**	1.585	3.3	1.01	**6.20**	1.19	6.07	1.02
Eu	35.6	**0.527**	0.84	0.53	0.99	**1.47**	1.68	1.53	0.96	**1.09**	1.196	1.08	1.01	**2.04**	0.53	2.07	0.99
Gd	37.3	**1.81**	1.36	1.87	0.97	**4.26**	1.27	4.52	0.94	**3.61**	1.071	3.66	0.99	**6.04**	0.24	6.24	0.97
Tb	37.6	**0.347**	0.72	0.36	0.96	**0.582**	1.55	0.64	0.91	**0.585**	0.97	0.62	0.94	**0.896**	1.15	0.92	0.97
Dy	35.5	**2.51**	1.98	2.51	1.00	**3.31**	0.86	3.47	0.95	**3.76**	0.971	3.79	0.99	**5.13**	1.39	5.31	0.97
Ho	38.3	**0.558**	1.47	0.56	1.00	**0.639**	1.67	0.65	0.98	**0.769**	0.832	0.79	0.97	**0.957**	1.25	0.98	0.98
Er	38	**1.68**	1.71	1.66	1.01	**1.73**	2.34	1.81	0.96	**2.19**	0.693	2.22	0.99	**2.48**	1.68	2.54	0.98
Yb	39.2	**1.66**	1.14	1.65	1.01	**1.59**	2.16	1.62	0.98	**2.09**	2.152	2.05	1.02	**1.99**	1.13	2	0.99
Lu	37	**0.240**	1.95	0.25	0.96	**0.233**	1.73	0.247	0.94	**0.296**	1.788	0.31	0.96	**0.268**	1.68	0.274	0.98
Average			2.25		1.02		1.36		0.97		1.14		0.98		1.15		0.98

Supplementary Table DR3: Major and trace element compositions of mafic rocks from the Innersuartuut.

	G93-138	G93-144	G93-145	G93-146	JG03/29	JG03/30	JG03/31	JG03/27	G93-140	JG03/32	G93-143
	Subalkalic Basalts				Cumulates				Outliers		
SiO_2	50.5	50.8	51.7	50.7	50.0	48.4	50.5	44.1	49.7	48.2	49.1
TiO_2	1.70	1.31	1.15	1.37	0.54	0.82	0.56	0.36	0.66	0.583	1.98
Al_2O_3	14.27	11.21	10.56	10.99	5.98	8.34	7.23	4.97	4.54	7.337	14.29
FeO_{tot}	18.4	15.2	14.6	15.4	13.4	15.7	12.7	12.9	16.6	14.3	19.7
MnO	0.23	0.21	0.21	0.22	0.26	0.24	0.22	0.24	0.33	0.221	0.23
MgO	4.8	8.1	8.4	7.4	15.0	13.6	13.1	22.3	13.6	16.2	5.2
CaO	6.3	9.1	9.3	9.9	14.0	11.9	12.3	11.2	13.2	10.4	5.6
Na_2O	3.00	2.59	2.42	2.54	1.03	1.30	1.44	0.70	1.02	0.803	3.32
K_2O	0.72	1.14	0.50	0.46	0.32	0.44	0.87	0.27	0.26	1.722	0.69
P_2O_5	0.09	0.09	0.10	0.09	0.04	0.06	0.04	0.03	0.19	0.045	0.10
Sum	100.0	99.8	98.8	99.0	100.5	100.8	99.0	98.7	100.2	99.5	100.1
Sc	27.5	32.8	33.5	35.2	46.8	46.6	43.8	21.5	46.0	34.8	26.6
Ti	10057	7703	6772	7922	3218	5026	3286	2091	3848	3351	11585
Cr	14	221	291	137	2091	1175	1731	3853	1319	1853	11
Ni	42	154	157	119	337	308	283	1422	307	470	53
Rb	5.8	72.5	12.3	8.2	3.7	5.9	61.5	4.5	5.5	103.8	5.9
Sr	319	105	104	102	67.1	64.5	56.4	16.3	27.3	13.7	209
Y	28.6	24.2	21.0	23.7	15.0	20.7	16.7	9.7	51.5	12.7	27.7
Zr	89.8	78.0	79.6	66.4	24.9	38.7	30.2	22.8	45.9	31.4	76.8
Nb	5.36	3.52	2.95	3.23	1.39	1.78	1.16	0.74	3.43	0.95	6.41
Ba	73.6	109	73.9	42.0	7.4	32.3	49.8	2.9	25.6	33.9	103
Hf	2.50	2.34	2.34	2.00	0.85	1.30	0.94	0.70	1.62	1.09	2.23
Ta	0.300	0.214	0.199	0.211	0.122	0.099	0.083	0.064	0.214	0.082	0.286
Th	0.087	0.079	0.098	0.102	0.120	0.037	0.064	0.311	0.172	0.089	0.102
U	0.040	0.043	0.056	0.030	0.020	0.042	0.023	0.103	0.042	0.044	0.052
La	7.85	5.80	5.05	5.90	3.59	4.35	4.02	1.73	12.64	2.87	13.16
Ce	22.98	18.05	14.99	17.55	11.15	13.69	11.52	4.06	40.10	7.15	37.32
Pr	3.60	2.94	2.43	2.83	1.67	2.16	1.72	0.59	6.45	0.983	5.55
Nd	18.2	15.5	12.3	14.1	7.26	10.3	7.96	2.93	31.2	4.36	26.5
Sm	5.65	4.76	3.96	4.65	1.98	3.11	2.43	1.10	9.97	1.54	6.81
Eu	1.79	1.34	1.20	1.42	0.511	0.804	0.576	0.287	1.11	0.512	1.54
Gd	6.21	5.25	4.64	5.13	2.48	3.66	2.88	1.46	10.9	2.12	6.64
Tb	1.131	0.948	0.855	0.920	0.493	0.694	0.542	0.303	1.964	0.391	1.134
Dy	5.99	4.94	4.45	4.96	2.83	3.79	3.27	1.73	10.68	2.44	5.83
Ho	1.18	1.00	0.882	0.96	0.590	0.823	0.640	0.377	2.04	0.505	1.14
Er	3.35	2.74	2.40	2.71	1.66	2.35	1.82	1.17	5.52	1.47	3.21
Yb	2.93	2.39	2.17	2.34	1.65	2.11	1.58	0.936	4.63	1.32	3.00
Lu	0.398	0.336	0.292	0.308	0.213	0.292	0.238	0.142	0.602	0.188	0.443

Assessment of alteration and secondary element mobility

Previous studies of Eoarchean mafic rocks have shown that element mobility can overprint original geochemical compositions, complicating petrological interpretations (Polat et al., 2002; Polat and Hofmann, 2003; Polat et al., 2003; Jenner et al., 2009). However, carefully focusing on selection of samples devoid of obvious signs of secondary alteration, such as silica and carbonate veining, can yield samples with only minor post-magmatic alteration (Frei and Jensen, 2003; Jenner et al., 2009). Various methods can be used to assess the degree of post-magmatic element mobility within Archean mafic rocks and are considered a prerequisite to any petrological interpretations.

Major element contents of samples from Innersuartuut (Supplementary Table 3) show systematic variations with decreasing MgO, indicating minimal post-magmatic alteration (Supplementary Fig. 2). Previous contributions have used the correlation coefficient (R^2) between element x and Zr (considered one of the least mobile trace elements during post-magmatic alteration) to identify samples that have sustained post magmatic alteration (Polat et al., 2002; Polat and Hofmann, 2003); this approach is applicable only if volcanic samples are cogenetic, or at least share a similar petrogenesis. Samples within a selected suite of amphibolites with an R^2 of <0.75 for a number of elements are considered by Polat and Hofmann (2003) as variably altered and not used for petrological interpretations. Variations in TiO_2, Al_2O_3, MgO, CaO and Na_2O versus Zr for all samples have an R^2 >0.7 (Supplementary Figs. 3 and 4; values in grey referred to as 'all basalts'). However, JG03/32 has anomalously high K_2O and G93/140 has considerably higher P_2O_5, and lower Al_2O_3 at a given MgO content compared to the other samples from Innersuartuut (Supplementary Fig. 2; discriminated from other samples as

crosses and referred to as ‘geochemical outliers’), suggesting these samples are not cogenetic with the remainder of the Innersuartuut suite or are variably altered. Additionally, sample G93/143 is an outlier on the plots of TiO_2, Al_2O_3, CaO and Na_2O versus Zr (Supplementary Fig. 3).

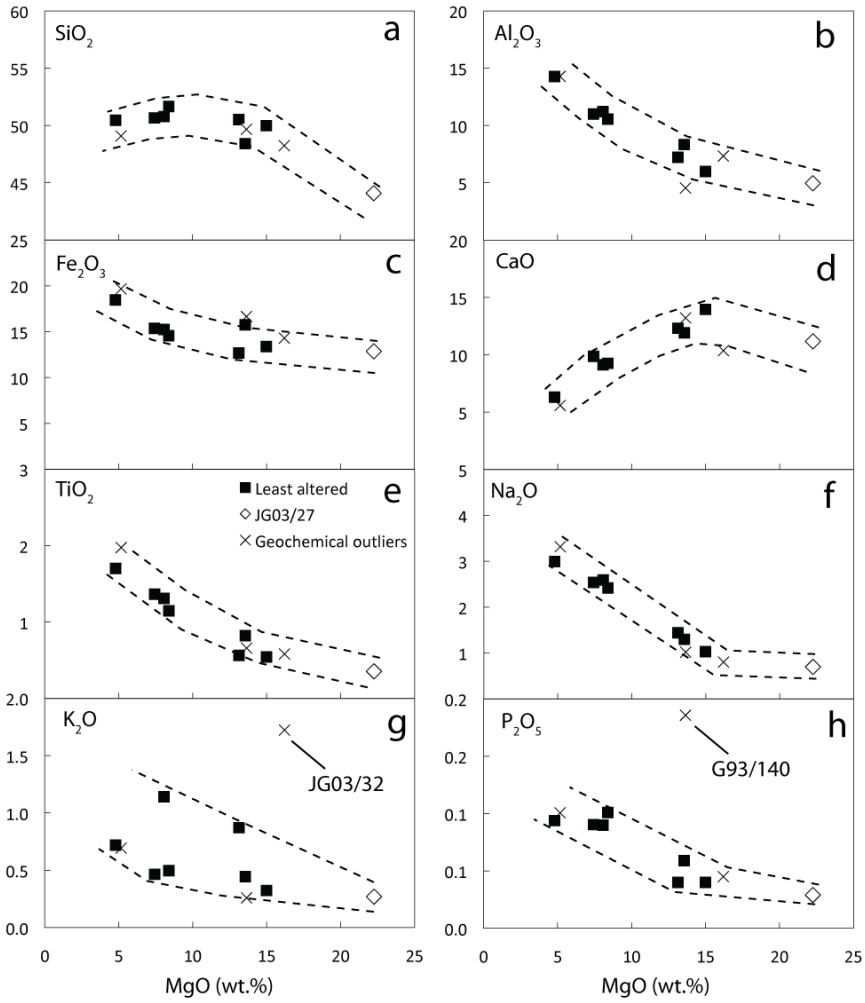

Supplementary Figure DR2: Covariation diagrams showing systematic variations in major elements versus MgO for samples from Innersuartuut. Coherent trends between major element versus MgO demonstrate that the effects of post magmatic alteration are minimal. The inflection in the trend of CaO versus MgO is consistent with clinopyroxene fractionation from the evolving melt. Samples labeled ‘geochemical outliers’ are samples with major and/or trace element compositions distinct from other samples in the suite. Samples labeled ‘least altered’ and sample JG03/27 are used to petrological interpretations.

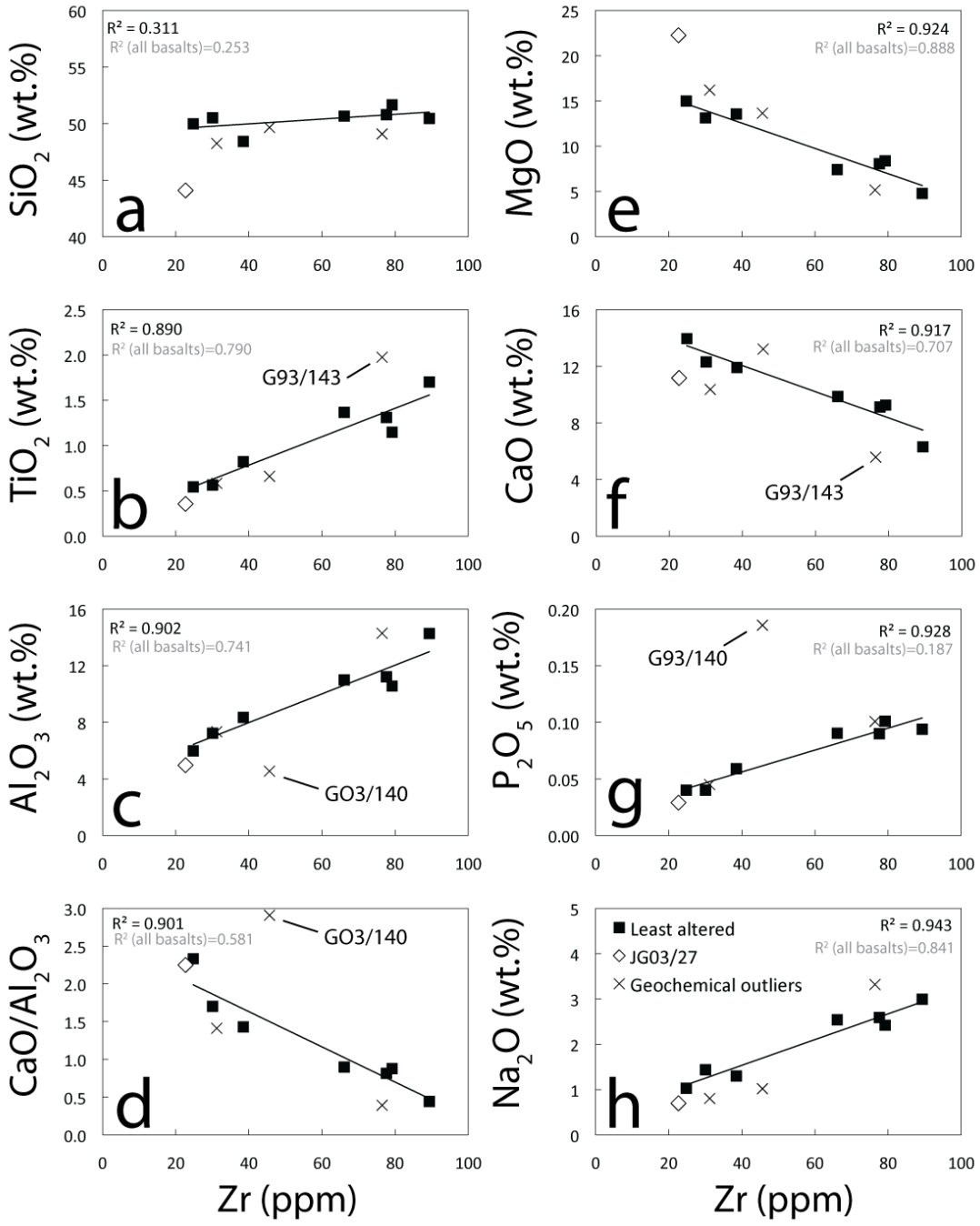

Supplementary Figure DR3: Covariation diagrams of major elements versus Zr for samples from Innersuartuut. High R2 values for least altered samples (values in black text; omitting samples G03/140, G93/143 and JG03/32) demonstrate that the major element chemistry of the Innersuartuut samples suffered only minimal effects of post-magmatic alteration. R2 calculated using all samples given in grey text.

Recalculation of R^2 omitting samples G93/143, JG03/32 and G03/140 (values in black, Supplementary Fig. 3 and 4), gives a considerably better fit for each of the major elements versus Zr, in particular, P_2O_5 versus Zr increases from 0.187 to 0.928. Similarly, calculation of R^2 for trace elements versus Zr are significantly higher (e.g., Yb, Y and Eu/Eu* increase from 0.139 to 0.784, 0.083 to 0.789 and 0.168 to 0.861, respectively), omitting samples G93/143, JG03/32 and G03/140 (Supplementary Fig. 4).

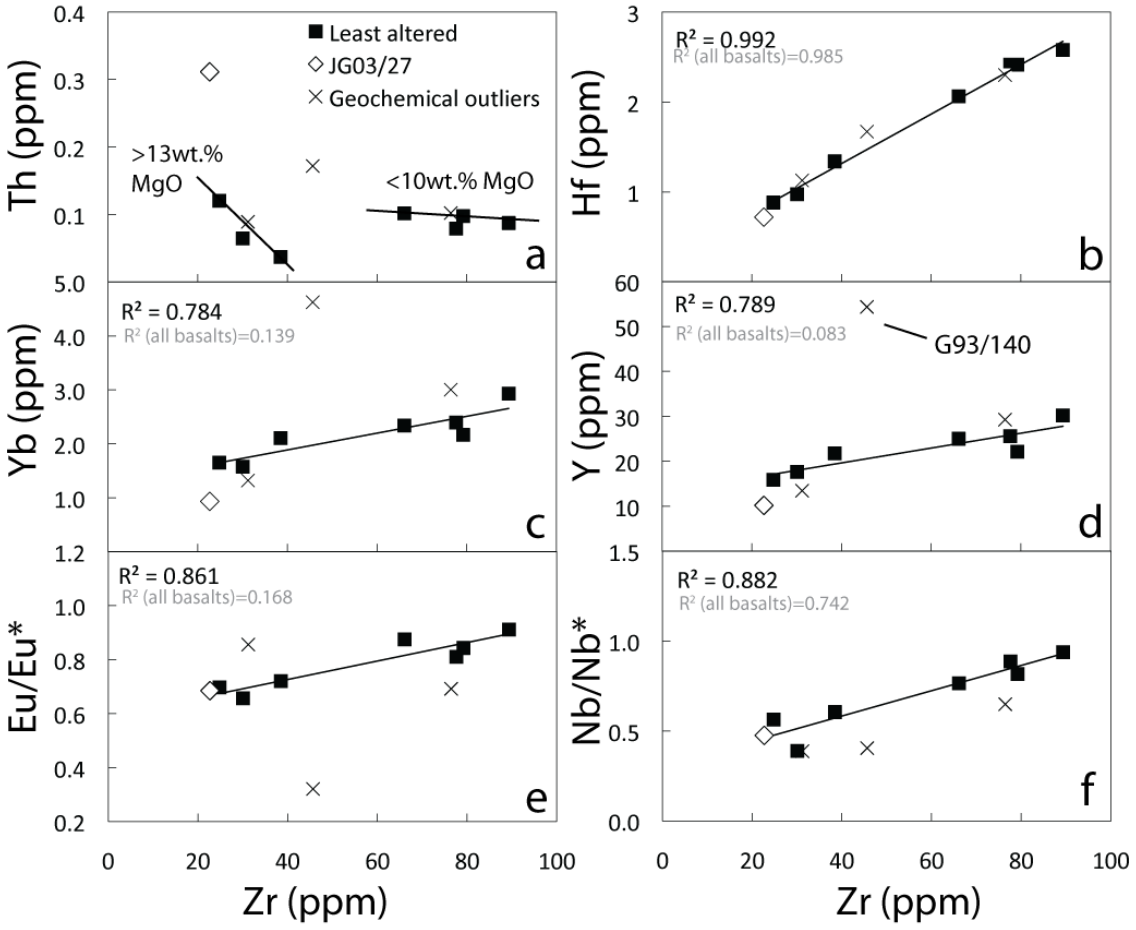

Supplementary Figure DR4: Trace element variations versus Zr for samples from Innersuartuut. Values in black are for the samples used for petrological interpretations. Element anomalies calculated using the methods described in Niu et al., (2009) for Eu/Eu* and Fan and Kerrich (1997) for Nb/Nb*.

Thus, samples G93/143, JG03/32 and G03/140 are considered 'variably altered' using the data filtering method of Polat et al.(2002) and are not used for further petrological interpretations in this contribution. However, the differences in chemistry of G93/143, JG03/32 and G03/140 with regards to geochemical trends may also be attributable to minor differences in petrogenesis and/or modal abundances of phases, which unfortunately with regards to the limited outcrops on Innersuartuut, cannot be determined without a greater number of samples. Thus, the term 'geochemical outlier' is considered here more appropriate than 'variably altered'. Variations in Th contents do not show a linear correlation with variations in Zr content (Supplementary Fig. 4a); samples with >10 wt.% MgO (<40 ppm Zr) show an increase in Th with decreasing Zr, whereas the samples with <10 wt.% MgO (>60 ppm Zr) display almost constant Th contents, indicating that either Th was not acting as an incompatible element or the primary igneous Th contents were overprinted by secondary alteration. However, the systematic behavior of Th in samples grouped together according to MgO content (either >10wt.% or <10 wt.% MgO) and the high R^2 between elements that are more prone to alteration than Th (e.g., CaO, P_2O_5 and Na_2O) indicate that this may be a primary feature of the Innersuartuut suite. Additionally, the coherent depletion trend with Nb>U>Th on primitive mantle normalized plots (Fig. 4) and systematic variations in elemental ratios suggests only minimal post-magmatic alteration or element mobility. Similarly, the high R^2 of the majority of samples from Innersuartuut, and for many elements typically considered extremely mobile during metamorphic/metasomatic alteration (e.g., CaO, P_2O_5 and Na_2O have an R^2 of 0.901, 0.928 and 0.943, respectively), supports our interpretation that these samples have suffered only minimal post-magmatic alteration.

Thus, the Innersuartuut suite provides an ideal opportunity to correlate the behavior of the major elements with the trace elements during petrological processes.

Comparison of innersuartuut suite with other archean mafic and ultramafic suites

In contrast to samples from Isua and Nuvvuagittuq, the Innersuartuut subalkalic basalts, plot slightly below, whereas the pyroxenitic basalts plot within the MORB-OIB array (Supplementary Fig. 5a) and show no evidence for a subduction-related input to their mantle source region. Nb/Yb versus Th/Yb provides an easy method for demonstrating the similarity in compositions of the Innersuartuut suite with the modern MORB-OIB array. However, the differences in compatibilities of Nb, Yb and Th during partial melting and fractional crystallization complicates the reliability of this method for gaining direct insights into the composition of the mantle source region (Hofmann et al., 1986). It is typically considered that a more rigorous test is to use elemental ratios that are uniform in all types of oceanic basalts (MORB and OIB), such as Nb/Th and Nb/U, and are considered to be relatively unfractionated by varying degrees of partial melting, source depletion and/or magma chamber processes (Hofmann et al., 1986; Palme and O'Neill, 2003). As such, the element ratios of the basalts are considered to reflect the ratios in the mantle source. However, the Innersuartuut suite show a range in both Nb/Th and Nb/U with increasing Nb (Supplementary Fig. 5c and d), demonstrating that these ratios are not as immune to the effects of pervasive clinopyroxene fractionation as we would like to believe. Similarly, unlike typical OIB, we find rare within-plate ankaramites from the Caribbean-Colombian plateau (Mamberti et al., 2003) and Hawaii (Frey et al., 1990; Frey et al., 1991), which all fractionate high percentages of clinopyroxene in crustal magma chambers, also plot within and outside of the MORB-OIB array with regards to Th/Yb versus Nb/Yb, and between Nb/Th and Nb/U versus Nb (Fig. 5), demonstrating similarities in their petrogenesis to the Innersuartuut suite during differentiation.

Differentiation in a crustal magma chamber often leads to assimilation of the host rock. However, the compositional trend resulting from clinopyroxene fractionation (shown on Supplementary Fig. 5) is contrary to that expected from crustal contamination

by a felsic end-member composition. Either the host rock was basaltic in composition or there was little assimilation. From major and trace element systematics and constraints from experimental petrology on the likely [MgO] of basaltic melts (O'Hara, 1968), we can infer that the composition of the parental magma of the Innersuartuut suite was likely intermediate between the subalkaline and the pyroxenitic basalts (Supplementary 5), and was comparable to the samples defining the modern MORB-OIB array with regards to Nb-Yb-Th-U systematics.

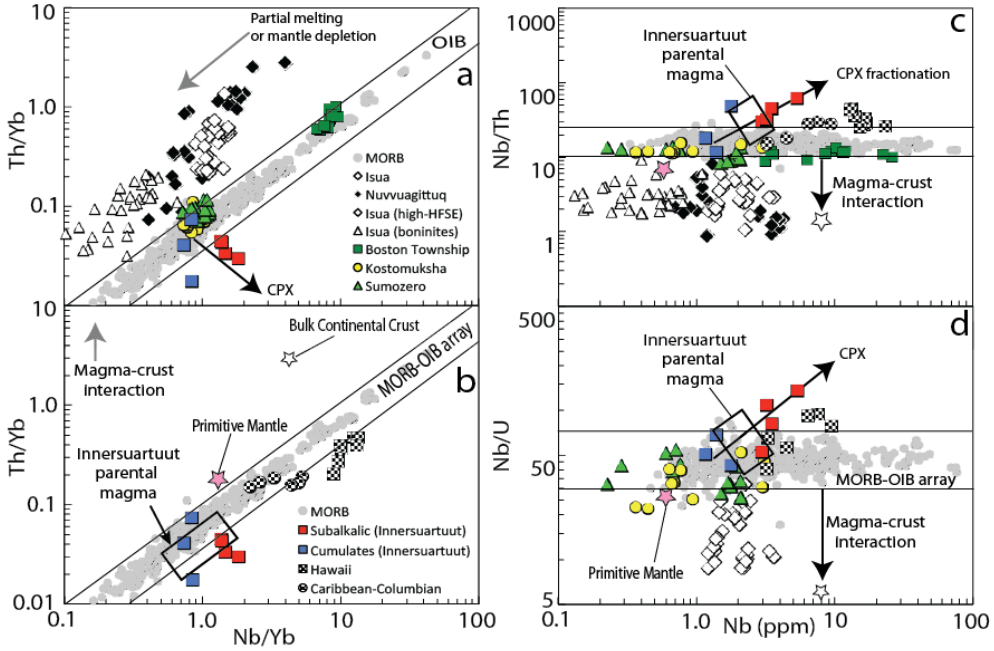

Supplementary Figure DR5: Nb-Yb-Th-U diagrams (Hofmann et al., 1986; Pearce, 2008) showing the compositions of the Innersuartuut subalkalic and pyroxenitic basalts compared to ancient mafic rocks from Isua (Polat et al., 2002; Polat and Hofmann, 2003; Polat et al., 2003; Jenner et al., 2009). Data from Jenner et al. (2009) were recalibrated using a new compilation of NIST SRM 612 values presented in Jenner and O'Neill (2012b), Nuvvuagittuq (O'Neil et al., 2011), and Mesoarchean rocks; ~2.8 Ga Kostomuksha (Puchtel et al., 1998) and 2.9 Ga Sumozero-Kenozero (Puchtel et al., 1999) GSB of the Baltic Shield, and ~2.7 Ga Boston Township komatiites and tholeiites from the Abitibi GSB (Xie and Kerrich, 1994) and modern modern within-plate ankaramites from the Caribbean-Columbian plateau (Mamberti et al., 2003) and Mauna Kea, Hawaii (Frey et al., 1990; Frey et al., 1991). MORB array; Jenner and O'Neill (2012a); bulk continental crust; from Rudnick and Gao (2003) and primitive mantle from Palme and O'Neill (2003). The trends in compositions of the Innersuartuut suite are consistent with cpx fractionation and are contrary to the trends expected for crustal assimilation of a felsic composition and/or a subduction-related petrogenesis. The composition of the parental magma of the Innersuartuut suite (open boxes) is likely intermediate between the compositions of the most mafic subalkalic basalts and the pyroxenitic basalts.

REFERENCES CITED

Fan, J., and Kerrich, R., 1997, Geochemical characteristics of aluminum depleted and undepleted komatiites and HREE-enriched low-Ti tholeiites, western Abitibi greenstone belt; a heterogeneous mantle plume-convergent margin environment: Geochimica et Cosmochimica Acta, v. 61, p. 4723-4744.

Frei, R., and Jensen, B. K., 2003, Re-Os, Sm-Nd isotope- and REE systematics on ultramafic rocks and pillow basalts from the Earth's oldest oceanic crustal fragments (Isua supracrustal belt and Ujaragssuit nunat area, W Greenland): Chemical Geology, v. 196, p. 163-191.

Frey, F. A., Garcia, M. O., Wise, W. S., Kennedy, A., Gurriet, P., and Albarede, F., 1991, The evolution of Mauna Kea Volcano, Hawaii; petrogenesis of tholeiitic and alkalic basalts: Journal of Geophysical Research, B, Solid Earth and Planets, v. 96, p. 14,347-314,375.

Frey, F. A., Wise, W. S., Garcia, M. O., West, H. B., Kwon, S.-T., and Kennedy, A., 1990, Evolution of Mauna Kea Volcano, Hawaii: Petrologic and Geochemical Constraints on Postshield Volcanism: Journal of Geophysical Research, v. 95, p. 1271-1300.

Hofmann, A. W., Jochum, K. P., Seufert, M., and White, W. M., 1986, Nb and Pb in oceanic basalts: new constraints on mantle evolution: Earth and Planetary Science Letters, v. 79, no. 1-2 SU -, p. 33-45.

Jenner, F. E., Bennett, V. C., Nutman, A. P., Friend, C. R. L., Norman, M. D., and Yaxley, G., 2009, Evidence for subduction at 3.8 Ga: Geochemistry of arc-like metabasalts from the southern edge of the Isua Supracrustal Belt: Chemical Geology, v. 261, p. 83-98.

Jenner, F. E., and O'Neill, H. s. C., 2012a, Analysis of 60 Elements in 616 Ocean Floor Basaltic Glasses: Geochemistry Geophysics Geosystems, v. 13, no. 1, p. Q02005.

-, 2012b, Major and trace analysis of basaltic glasses by laser-ablation ICP-MS: Geochemistry Geophysics Geosystems, v. 13, no. 3.

Jochum, K. P., Nohl, L., Herwig, K., Lammel, E., Stoll, B., and Hofmann, A. W., 2005, GeoReM: A new geochemical database for reference materials and isotopic standards: Geostandards and Geoanalytical Research, v. 29, no. 3, p. 333-338.

Mamberti, M., Lapierre, H., Bosch, D., Jaillard, E., Ethien, R., Hernandez, J., and Polve, M., 2003, Accreted fragments of the Late Cretaceous Caribbean-Colombian Plateau in Ecuador: Lithos, v. 66, no. 3-4, p. 173-199.

Niu, Y., and O'Hara, J., 2009, MORB mantle hosts the missing Eu (Sr, Nb, Ta and Ti) in the continental crust: New perspectives on crustal growth, crust–mantle differentiation and chemical structure of oceanic upper mantle: Lithos, v. 112, no. 1-2, p. 1-17.

Nutman, A. P., McGregor, V. R., Shiraishi, K., Friend, C. R. L., Bennett, V. C., and Kinny, P. D., 2002, ≥3850 Ma BIF and mafic inclusions in the early Archaean Itsaq gneiss complex around Akilia, southern West Greenland? The difficulties of precise dating of zircon-free protoliths in migmatites: Precambrian Research, v. 117, p. 185-224.

O'Hara, M. J., 1968, Are ocean floor basalts primary magmas?: Nature, v. 220, p. 683-686.

O'Neil, J., Francis, D., and Carlson, R. W., 2011, Implications of the Nuvvuagittuq Greenstone Belt for the Formation of Earth's Early Crust: Journal of Petrology, v. 52, no. 5, p. 985-1009.

Palme, H., and O'Neill, H. s. C., 2003, Compositional Estimates of Mantle Composition, *in* Carlson, R. W., ed., The Mantle and Core, Volume 2: Elsevier-Pergamon, Oxford, p. 1-38.

Pearce, J. A., 2008, Geochemical fingerprinting of oceanic basalts with applications to ophiolite classification and the search for Archean oceanic crust: Lithos, v. 100, p. 14-48.

Polat, A., and Hofmann, A. W., 2003, Alteration and geochemical patterns in the 3.7-3.8 Ga Isua greenstone belt, West Greenland: Precambrian Research, v. 126, p. 197-218.

Polat, A., Hofmann, A. W., Muenker, C., Regelous, M., and Appel, P. W. U., 2003, Contrasting geochemical patterns in the 3.7-3.8 Ga pillow basalt cores and rims, Isua greenstone belt, Southwest Greenland; implications for postmagmatic alteration processes: Geochimica et Cosmochimica Acta, v. 67, p. 441-457.

Polat, A., Hofmann, A. W., and Rosing, M. T., 2002, Boninite-like volcanic rocks in the 3.7-3.8 Ga Isua greenstone belt, West Greenland; geochemical evidence for intra-oceanic subduction zone processes in the early Earth: Chemical Geology, v. 184, p. 231-254.

Puchtel, I. S., Hofmann, A. W., Amelin, Y. V., Garbe, S. C. D., Samsonov, A. V., and Shchipansky, A. A., 1999, Combined mantle plume-island arc model for the formation of the 2.9 Ga Sumozero-Kenozero greenstone belt, SE Baltic Shield; isotope and trace element constraints: Geochimica et Cosmochimica Acta, v. 63, p. 3579-3595.

Puchtel, I. S., Hofmann, A. W., Mezger, K., Jochum, K. P., Shchipansky, A. A., and Samsonov, A. V., 1998, Oceanic plateau model for continental crustal growth in the Archaean; a case study from the Kostomuksha greenstone belt, NW Baltic Shield: Earth and Planetary Science Letters, v. 155, p. 57-74.

Rudnick, R. L., and Gao, S., 2003, Composition of the Continental Crust, *in* Rudnick, R. L., ed., Treatise on Geochemistry, Volume 3: The Crust, Volume 3: Oxford, Elsevier, p. 1-64.

Xie, Q., and Kerrich, R., 1994, Silicate-perovskite and majorite signature komatiites from the Archean Abitibi greenstone belt; implications for early mantle differentiation and stratification: Journal of Geophysical Research, B, Solid Earth and Planets, v. 99, p. 15,799-715,812.